A variational method using Alpert multiwavelets

A. J. Stacey[1] W. F. Blyth[2]

(Received 7 August 2006; revised 27 November 2007)

Abstract

The numerical solution of variational problems is usually achieved by numerical solution of the Euler–Lagrange differential equations or by Rayleigh–Ritz direct methods. In 1975, Chen and Hsiao showed how Walsh functions could be used in a direct method to solve several model variational problems. This Rayleigh–Ritz method was generalized by Sloss and Blyth in 1998. In 2004, Hsiao modified the Walsh function method to provide a Haar wavelet direct method and illustrated how this could be used for the solution of a few model problems. We extend this by applying Alpert multiwavelets to the direct solution of variational problems. Alpert multiwavelets were developed for the numerical solution of integral equations and provide a generalization of Haar wavelets. Alpert multiwavelets have the advantage of being expressible as simple polynomials over disjoint subintervals allowing

See http://anziamj.austms.org.au/ojs/index.php/ANZIAMJ/article/view/73 for this article, Published January 3, 2008. ISSN 1446-8735

for ease of computation. The method is applied to an example which allows comparisons with the results for Haar wavelets to be made. Some convergence results are given.

Contents

1 Introduction

Alpert multiwavelets [1] were developed in 1990 to provide sparse representations of integral operators for the solution of integral equations. Recently they have been successfully used to solve partial differential equations [2]. Alpert multiwavelets generalize Haar wavelets and consist of piecewise polynomial functions; rather than the irregularly shaped Daubechies wavelets [5]

which also generalize Haar wavelets.

The basic idea of a direct method in variational problems is to convert an infinite dimensional problem into a finite dimensional problem by expressing the unknown solution function as a finite series expansion in some set of basis functions.

Many different basis sets have been used [8]. Walsh functions were used by Chen and Hsiao [4]. This approach was generalized by Sloss and Blyth [9]. Other approaches using globally defined functions include Hwang and Shih [7], who used Laguerre functions. Locally defined functions—nonzero only on a subinterval—include the Shifted Legendre functions used by Chang and Wang [3]. More recently, in 2004 Hsiao [6] modified the Walsh function approach and used Haar wavelets.

Although Haar wavelets have some computational advantages they are slow to converge and produce solutions which are piecewise constant. Alpert multiwavelets have the advantage of converging more rapidly and produce piecewise polynomial solutions of any order. Multiwavelets have not been used previously for solving variational problems.

2 Alpert multiwavelets

2.1 Haar wavelets

The Haar wavelets form an orthonormal basis for $L_2([0,1))$ and consists of a single scale function $S(t)$ plus wavelets $H_{n,\ell}(t)$ defined below. Note that all these functions are normalized.

The scale function is

$$S(t) = \begin{cases} 1, & \text{if } 0 \leqslant t < 1\,, \\ 0, & \text{otherwise,} \end{cases}$$

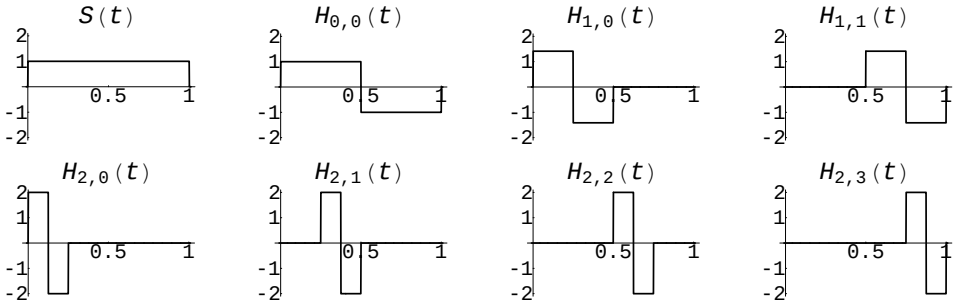

FIGURE 1: The scale function (top left hand function) followed by the first seven Haar wavelets.

whereas the wavelets are

$$H_{n,\ell}(t) = 2^{n/2} H(2^n t - \ell)\,,$$

where the function $H(t)$, the mother wavelet, is

$$H(t) = \begin{cases} 1, & \text{if } 0 \leqslant t < \frac{1}{2}\,, \\ -1, & \text{if } \frac{1}{2} \leqslant t < 1\,, \\ 0, & \text{otherwise,} \end{cases}$$

with $n = 0, 1, 2, \ldots$ and $\ell = 0, \ldots, 2^n - 1$. Note that the support for $H_{n,\ell}(t)$ is the interval $[2^{-n}\ell, 2^{-n}(\ell + 1))$. The first eight terms of the Haar basis are shown in Figure 1.

In applications, functions are approximated by a Fourier-wavelet series which is truncated to the series with the scale function(s) and all wavelets up to the given level n. For the case of the Haar wavelets, there is one scale function with a total of $m = 2^{n+1}$ terms in the truncated series.

2.2 Alpert wavelets

Alpert multiwavelets generalize Haar wavelets by replacing the single scale function $S(t)$ by k scale functions $S^j(t)$, where $j = 0, 1, \ldots, k-1$, defined on $[0, 1)$. The functions $S^j(t)$ are derived from the first k Legendre polynomials $P_j(t)$ by rescaling, shifting and renormalizing so that $S^j(t)$ are defined on $[0, 1)$ rather than $[-1, 1)$ [2]. Note that the $S^j(t)$ functions form an orthonormal set and span the space of all polynomials of order up to $k-1$ on the interval $[0, 1)$.

Similarly we replace the single wavelet $H_{0,0}(t) = H(t)$ on $[0, 1)$ by k orthonormal wavelets $A^j_{0,0}(t) = A^j(t)$ on $[0, 1)$, where $j = 0, 1, \ldots, k-1$. The Alpert wavelets are then

$$A^j_{n,\ell}(t) = 2^{n/2} A^j(2^n t - \ell)\,,$$

where the functions $A^j(t)$ are defined below and where $n = 0, 1, 2, \ldots$ and $\ell = 0, 1, \ldots, 2^n - 1$. Note that the interval $[2^{-n}\ell, 2^{-n}(\ell+1))$ is also the support for the $A^j_{n,\ell}(t)$ functions.

Going from Haar to Alpert we replace one function on each subinterval with a basis of k functions on each subinterval. An Alpert k wavelet series truncated to the level n has $m = k2^{n+1}$ terms.

The k wavelets $A^j(t)$ on $[0, 1)$ are required to be piecewise polynomial of order at most $k-1$ on each of the two subintervals $[0, 1/2)$ and $[1/2, 1)$. This requirement derives essentially from the multiresolution structure of the wavelet basis [10]. This means that there are $2k^2$ coefficients that need to be chosen to define the $A^j(t)$ functions. The only essential constraints are that the $2k$ functions $\{A^j(t), S^j(t)\}$ form an orthonormal set. However, this does not provide enough constraints to determine the polynomial coefficients uniquely. Alpert makes some special choices which give the polynomials up to a choice of sign [1] and it is these polynomials which we use.

2.3 Alpert $k = 2$

The first two scale functions, which are essentially Legendre polynomials, are

$$S^0(t) = \begin{cases} 1, & \text{if } 0 \leqslant t \leqslant 1\,, \\ 0, & \text{otherwise,} \end{cases}$$

and

$$S^1(t) = \begin{cases} \sqrt{3}(1-2t), & \text{if } 0 \leqslant t \leqslant 1\,, \\ 0, & \text{otherwise.} \end{cases}$$

The corresponding Alpert wavelets $A^0(t) = A^0_{0,0}(t)$ and $A^1(t) = A^1_{0,0}(t)$ are

$$A^0(t) = \begin{cases} -\sqrt{3}(4t-1), & \text{if } 0 \leqslant t \leqslant 1/2\,, \\ \sqrt{3}(4t-3), & \text{if } 1/2 < t \leqslant 1\,, \end{cases}$$

and

$$A^1(t) = \begin{cases} 6t-1\,, & \text{if } 0 \leqslant t \leqslant 1/2\,, \\ 6t-5\,, & \text{if } 1/2 < t \leqslant 1\,. \end{cases}$$

The first 16 terms of the Alpert wavelets basis, with $k = 2$, are given in Figure 2. Any function which is piecewise linear on the four subintervals of $[0, 1)$ can be expressed as a truncated series of these 16 wavelets.

2.4 Alpert $k = 3$

With $k = 3$ we just add the next shifted and rescaled Legendre polynomial

$$S^2(t) = \begin{cases} \sqrt{5}(6t^2-6t+1), & \text{if } 0 \leqslant t < 1\,, \\ 0, & \text{otherwise,} \end{cases}$$

and the three wavelets

$$A^0(t) = \begin{cases} -\frac{7}{3} + 24t - 40t^2\,, & \text{if } 0 \leqslant t \leqslant 1/2\,, \\ \frac{55}{3} - 56t + 40t^2\,, & \text{if } 1/2 < t \leqslant 1\,, \end{cases}$$

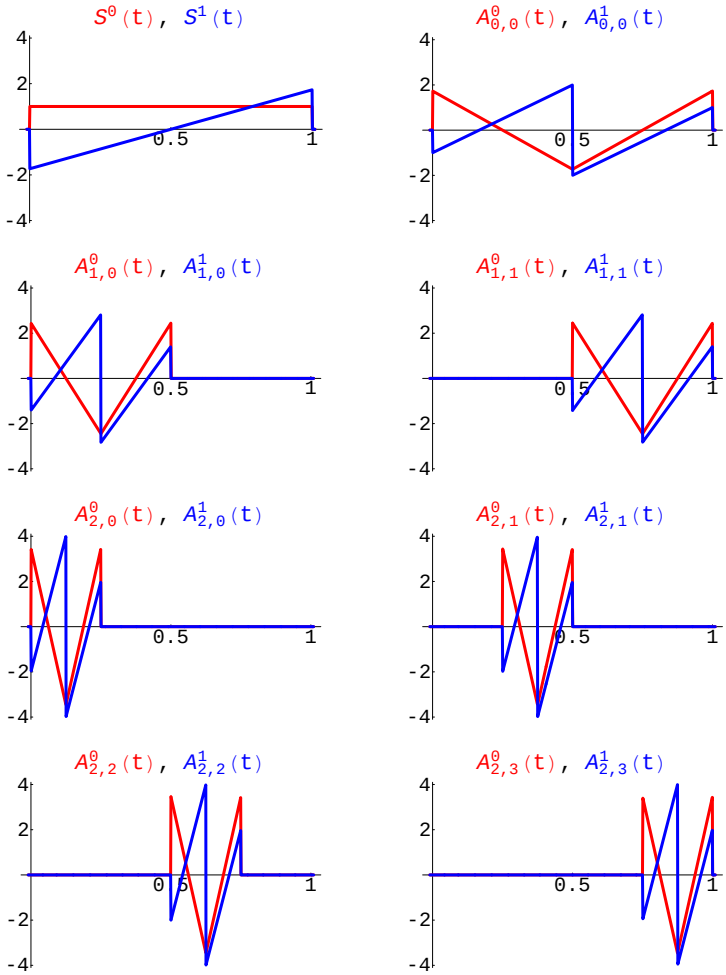

FIGURE 2: The first two Alpert ($k = 2$) scale functions (top left) plus the next 14 Alpert wavelets plotted in pairs.

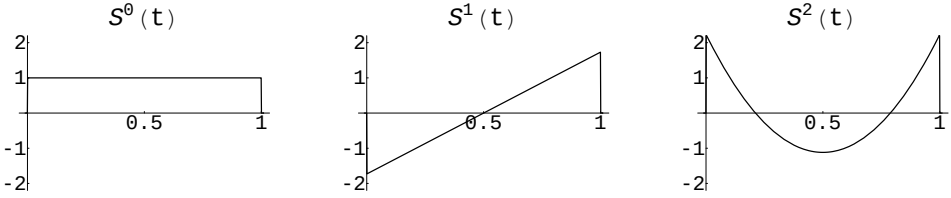

FIGURE 3: The first three Alpert ($k = 3$) scale functions.

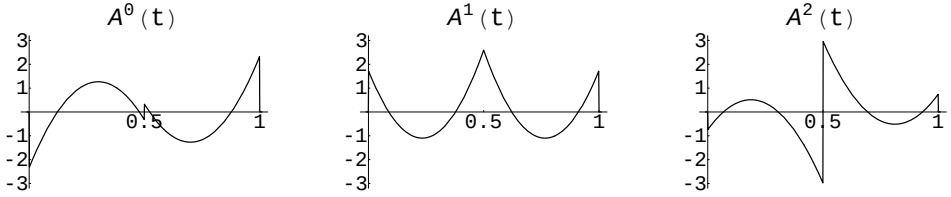

FIGURE 4: The first three Alpert ($k = 3$) wavelets.

$$A^1(t) = \begin{cases} \sqrt{3}(1 - 14t + 30t^2), & \text{if } 0 \leqslant t \leqslant 1/2\,, \\ \sqrt{3}(17 - 46t + 30t^2), & \text{if } 1/2 < t \leqslant 1\,, \end{cases}$$

$$A^2(t) = \begin{cases} -\sqrt{5}(\frac{1}{3} + 6t - 16t^2), & \text{if } 0 \leqslant t \leqslant 1/2\,, \\ \sqrt{5}(\frac{31}{3} - 26t + 16t^2), & \text{if } 1/2 < t \leqslant 1\,. \end{cases}$$

Note that we do not just add an extra wavelet when going from $k = 2$ to $k = 3$ but get three new wavelets, hence the $A^j(t)$ are a different functions for different choices of k. The first three Alpert scale functions and the first three Alpert wavelets are shown in Figures 3 and 4 respectively.

3 Variational problem

Find the function $x(t)$ that optimizes the functional

$$J = \int_0^1 \left[\dot{x}^2(t) - \frac{\pi^2}{4} x^2(t) \right] dt \,, \tag{1}$$

with $x(0) = 0$ and $x(1) = 1$. The exact solution is $x(t) = \sin(\pi t/2)$.

All the examples in Hsiao [6] are represented exactly by piecewise polynomials of order four or less. Since we want to demonstrate the convergence properties of the Alpert wavelet basis we choose an example for which the solution cannot be represented exactly by finite order piecewise polynomials.

4 Method of solution

- Write the highest derivative $\dot{x}(t)$ in terms of the basis functions, that is $\dot{x}(t) \approx \sum_{i=1}^{m} c_i e_i(t)$, where $e_i(t)$ are the functions of the wavelet basis: scale functions plus wavelets.
- Write $x(t)$ in the terms of the basis functions, that is $x(t) \approx \sum_{i=1}^{m} d_i e_i(t)$.
- Substitute these into Equation (1) and use the orthonormality conditions to get

$$J = \sum_i \left(c_i^2 - \frac{\pi^2}{4} d_i^2 \right) . \tag{2}$$

- Write the d_i coefficients in terms of c_i.

  First write $x(t)$ in terms of $\dot{x}(t)$ by

$$x(t) = x(0) + \int_0^t \dot{x}(u)\, du \,.$$

This is rewritten by using our approximation for $\dot{x}(t)$ and the initial condition $x(0) = 0$ to give

$$x(t) \approx \sum_i c_i \int_0^t e_i(u)\, du\,. \tag{3}$$

At this point we solve for c_1, which is the coefficient for $S^0(t)$, by noting that $\int_0^1 e_i(u)du = 0$ for all the basis functions except $S^0(t)$. This follows from the orthogonality of all the other basis functions to $S^0(t)$. From this we conclude that $x(1) = c_1 = 1\,.$

Now to write d_i in terms of the c_i we first need to project the integrals in Equation (3) onto the basis functions. That is

$$\int_0^t e_k(u)\, du \approx \sum_{i=1}^{m} A_{k,i} e_i(t)\,,$$

where

$$A_{k,i} = \int_0^1 \left[\int_0^t e_k(u)\, du\right] e_i(t)\, dt$$

is the matrix form of the integration projection operator.

Now we write

$$x(t) \approx \sum_k c_k \int_0^t e_k(u)\, du \approx \sum_i \Big(\sum_k c_k A_{k,i}\Big) e_i(t)\,,$$

hence $d_i = \sum_k c_k A_{k,i}\,.$

- Optimize J to find the c_i.

  Substitute the expression for d_i above back into Equation (2) to give

$$J = \sum_i c_i^2 - \frac{\pi^2}{4}\Big(\sum_k c_k A_{k,i}\Big)^2\,.$$

Use $c_1 = 1$ and solve the system of equations

$$\frac{\partial J}{\partial c_i} = 0\,,$$

where $i = 2, 3, \ldots, m$ to find the other c_i values.

The solution is then

$$x(t) = \sum_i \sum_k c_k A_{k,i} e_i(t)\,.$$

5 Results

We use the L_2 or Euclidean measure of error

$$E(n) = \sqrt{\int_0^1 [f_a(t) - f_e(t)]^2\, dt}\,,$$

where $f_a(t)$ is the approximate solution, $f_e(t)$ is the exact solution and 2^n is the number of subintervals that $[0, 1)$ is divided into at its finest level. Note that this is a global measure of error.

The order of convergence can be approximated by $\log_2[E(n)/E(n+1)]$. Increasing n by 1, halves the smallest subinterval that wavelets are defined over.

Table 1 gives the global error measures for a range of n values, number of subintervals for each of $k = 1$, 2 and 3 basis functions per sub interval. Approximations to the orders of convergence for the global error are given in Table 2. The table shows that the order of convergence for Haar wavelets approaches 1, for Alpert wavelets ($k = 2$) approaches 2, and for Alpert wavelets ($k = 3$) approaches 3.

TABLE 1: L_2 error for the first three levels of Alpert wavelets, where $k\,2^{n+1}$ is the number of basis functions.

	n	1	2	3	4
Haar	$k=1$	0.08105	0.04020	0.02000	0.01002
Alpert	$k=2$	0.004060	0.001015	0.000253	0.0000634
Alpert	$k=3$	0.0001347	0.00001685	0.000002107	0.0000002634

TABLE 2: Approximate order of global convergence for the first three levels of Alpert wavelets.

		$\log_2 \frac{E(1)}{E(2)}$	$\log_2 \frac{E(2)}{E(3)}$	$\log_2 \frac{E(3)}{E(4)}$
Haar	$k=1$	1.0116	1.0032	1.0008
Alpert	$k=2$	1.9990	1.9974	1.9999
Alpert	$k=3$	2.9986	2.9996	2.9999

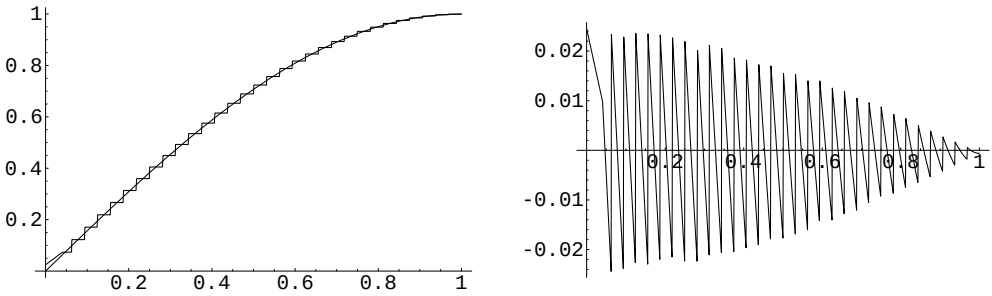

FIGURE 5: Haar $n = 4$ (32 basis functions). The first of the two plots shows both the approximate and exact solutions. The second plot show the error, $f_a(t) - f_e(t)$, as a function of t.

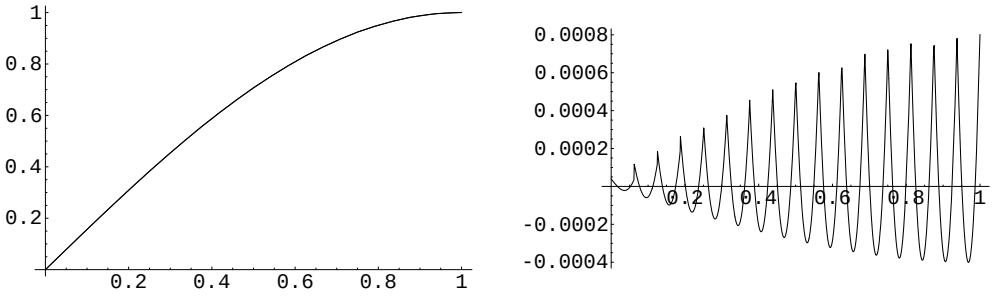

FIGURE 6: Alpert ($k = 2$) $n = 3$ (32 basis functions). The first of the two plots shows both the approximate and exact solutions. The second plot show the error, $f_a(t) - f_e(t)$, as a function of t.

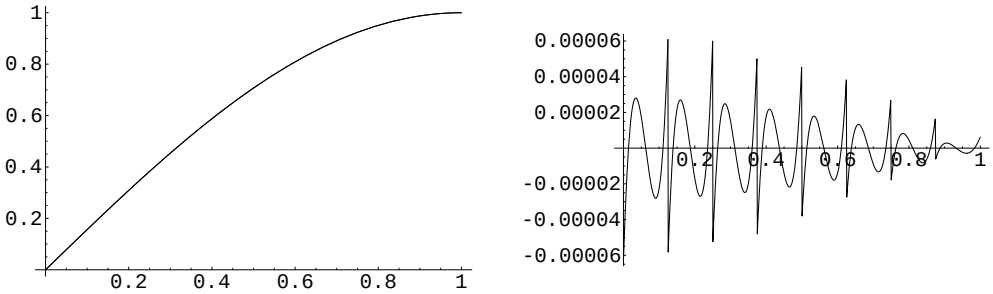

FIGURE 7: Alpert ($k = 3$) $n = 2$ (24 basis functions). The first of the two plots shows both the approximate and exact solutions. The second plot show the error, $f_a(t) - f_e(t)$, as a function of t.

A basis has $k2^{n+1}$ basis functions, where k is the number of basis functions per subinterval and 2^{-n} is the length of the smallest subinterval over which a basis function is non-zero. It is therefore not possible to make a straight comparison between different k values for the same n. To show that there is an advantage in using the Alpert wavelets a selection of k and n values has been made such that the number of basis functions is approximately the same. The following combinations were chosen for comparison. Haar $n = 4$, with 32 basis functions; Alpert $k = 2$ and $n = 3$, with 32 basis functions; and Alpert $k = 3$ and $n = 2$, with 24 basis functions. Table 2 shows that the Alpert wavelet schemes have the expected convergence orders and that for a similar (or reduced) computational cost, the higher order Alpert schemes provide greatly increased accuracy compared to the Haar scheme.

Figures 5, 6 and 7 show both the exact and approximate solutions, plotted on the same graph (the left hand graph), and the error as a function of t plotted on the right hand graph. Note that in Figures 6 and 7 there is no visible difference between the exact and approximate solutions.

6 Discussion

We have demonstrated the use of Alpert multiwavelets, which are a natural generalization of Haar wavelets, to successfully solve a variational problem, and confirmed the rates of convergence for different choices of the number of scale functions, k. The benefit of using these wavelets is the increased rate of convergence and much lower errors compared to Haar. The most expensive part of the calculation was the computation of the integration projection operator. In the calculations done for this paper they were done exactly using the symbolic capabilities of Mathematica. About 30% of the matrix entries were non-zero. Although an expensive computation it is only required to be calculated once and applied to a number of different problems. Finding symmetries and recursive definitions of this operator are currently under

investigation. Another problem that limits the application of this approach is being able to deal with functions of an unknown function, such as its cube or square root: further work is being directed to resolving this difficulty.

References

[1] B. K. Alpert. Sparse Representation of Smooth Linear Operators. PhD Thesis, Yale University, 1990. C821, C824

[2] B. K. Alpert, G. Beylkin, D. Gines and L. Vozovoi. Adaptive Solution of Partial Differential Equations in Multiwavelet Bases. *Journal of Computational Physics*, 182, 149–190, 2002. doi:10.1006/jcph.2002.7160 C821, C824

[3] R. Y. Chang and M. L. Wang. Shifted Legendre direct method for variational problems. *J. Optimization Theory Appl.*, 39, 299–307, 1983. C822

[4] C. F. Chen and C. H. Hsiao. A Walsh series direct method for solving variational problems. *J. Franklin Inst.*, 300, 265–280, 1975. C822

[5] I. Daubechies. Orthonormal bases of compactly supported wavelets. *Comm. Pure Appl. Math.*, 41(7), 909–996, 1988. C821

[6] C. H. Hsiao. Haar wavelet direct method for solving variational problems. *Mathematics and Computers in Simulation*, 64, 569–585, 2004. doi:10.1016/j.matcom.2003.11.012 C822, C828

[7] C. Hwang and Y. P. Shih. Laguerre series direct method for variational problems. *J. Optimization Theory Appl.*, 39, 143–149, 1983. C822

[8] R. S. Schechter. *The Variational Method in Engineering.* McGraw–Hill, NewYork, 1967. C822

[9] B. G. Sloss and W. F. Blyth. A variational method using Walsh functions. *Nonlinear Analysis, Theory, Methods and Applications*, 32, 549–561, 1998. C822

[10] D. F. Walnut. *An introduction to wavelet analysis*. Birkhäuser, Boston, 2002. C824

Author addresses

1. **A. J. Stacey**, School of Mathematical and Geospatial Sciences, RMIT University, Melbourne, AUSTRALIA.
mailto:astacey@rmit.edu.au

2. **W. F. Blyth**, School of Mathematical and Geospatial Sciences, RMIT University, Melbourne, AUSTRALIA.